SUMMER SCHOOL FOR HELIOPHYSICS

Radiation from Energetic Particles

T. S. Bastian
NRAO

Lecture Plan

- Overview of the electromagnetic spectrum
- Preliminaries
- Emission Mechanisms
  - Radio wavelengths
    - ✓ Gyrosynchrotron radiation
    - ✓ Plasma radiation
  - HXR/Gamma-ray energies
    - ✓ Nonthermal bremsstralung
    - ✓ Compton & Inverse Compton scattering
    - ✓ Pion decay
    - ✓ Annihilation radiation
    - ✓ Neutron capture
    - ✓ Nuclear excitation
- Examples (time permitting …)

WIND
Ulysses
Cassini
Stereo

NRH
Tremsdorf
Culgoora
Hiraiso
GB/SRBS
(FASR)

NoRH
OVSA
SSRT
VLA
BIMA
NoRP
(FASR)

JCMT
CSO
(ALMA)

Sac Peak
BBSO
La Palma
(ATST)
STEREO
Hinode
SDO

Yohkoh
SOHO
TRACE
STEREO
Hinode
SDO

Yohkoh
CGRO
RHESSI

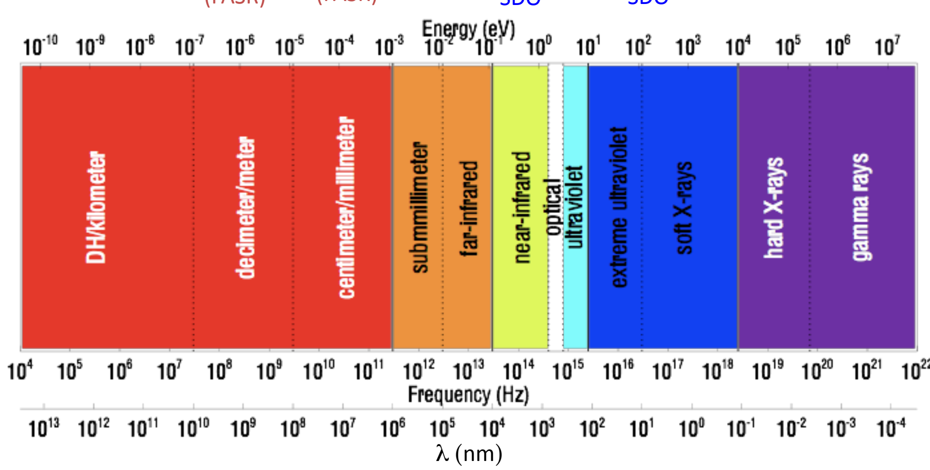

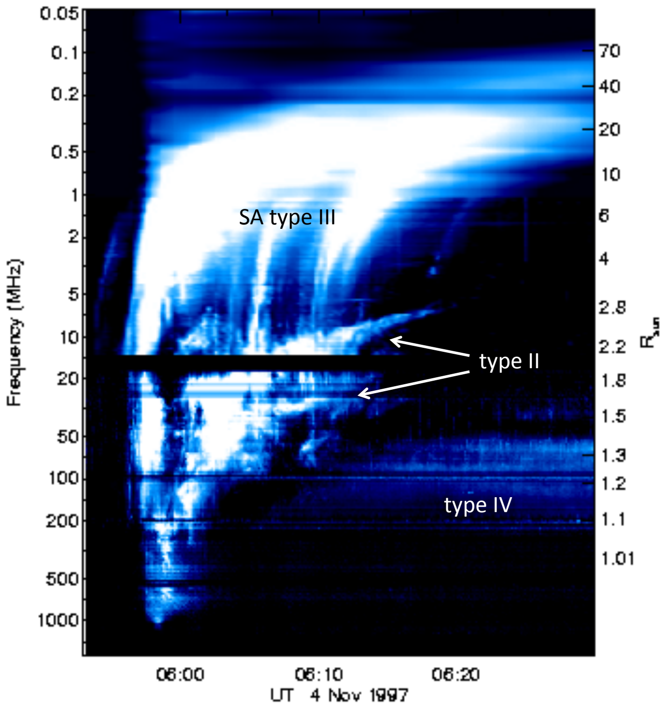
Frequency (MHz)
0.05
0.1
0.2
0.5
1
2
5
10
20
50
100
200
500
1000
70
40
20
10
6
4
2.8
2.2
1.8
1.5
1.3
1.2
1.1
1.01
R_{sun}
SA type III
type II
type IV
06:00
06:10
06:20
UT 4 Nov 1997

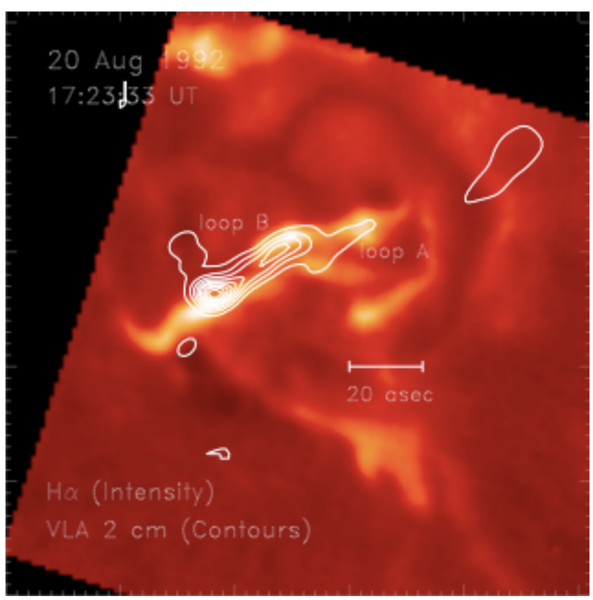
20 Aug 1992
17:23:33 UT
loop B
loop A
20 asec
Hα (Intensity)
VLA 2 cm (Contours)

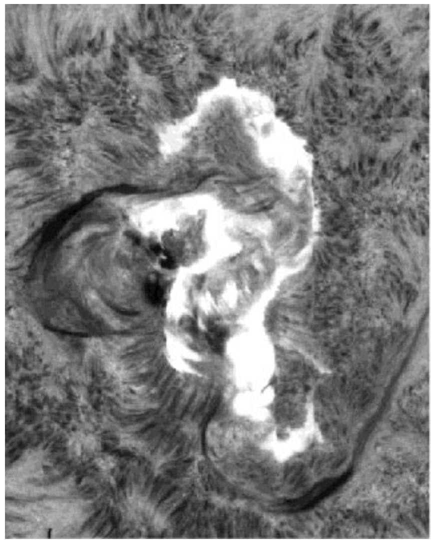

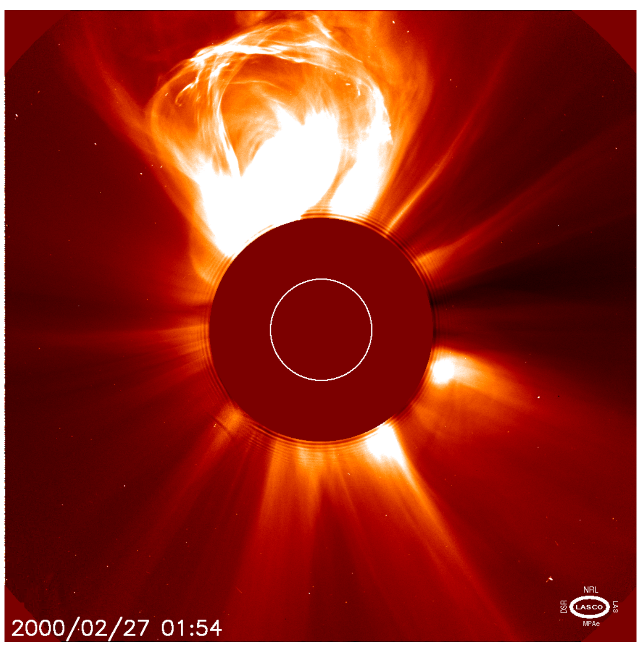
2000/02/27 01:54
NRL
LASCO
MPAe

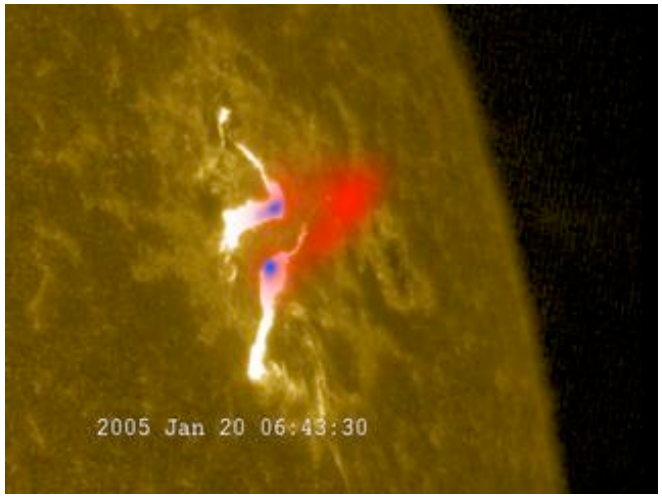
2005 Jan 20 06:43:30

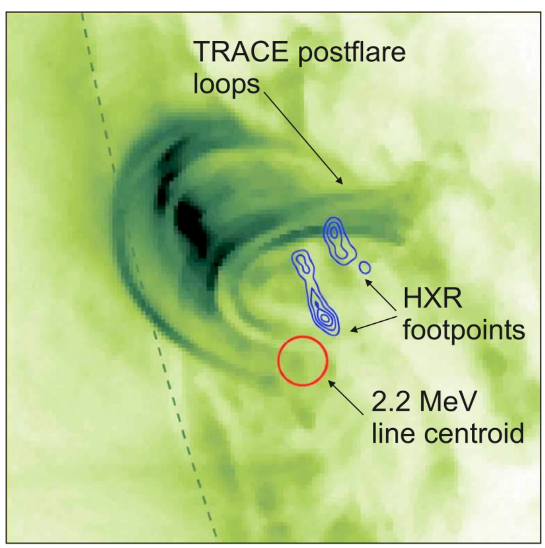
TRACE postflare loops
HXR footpoints
2.2 MeV line centroid

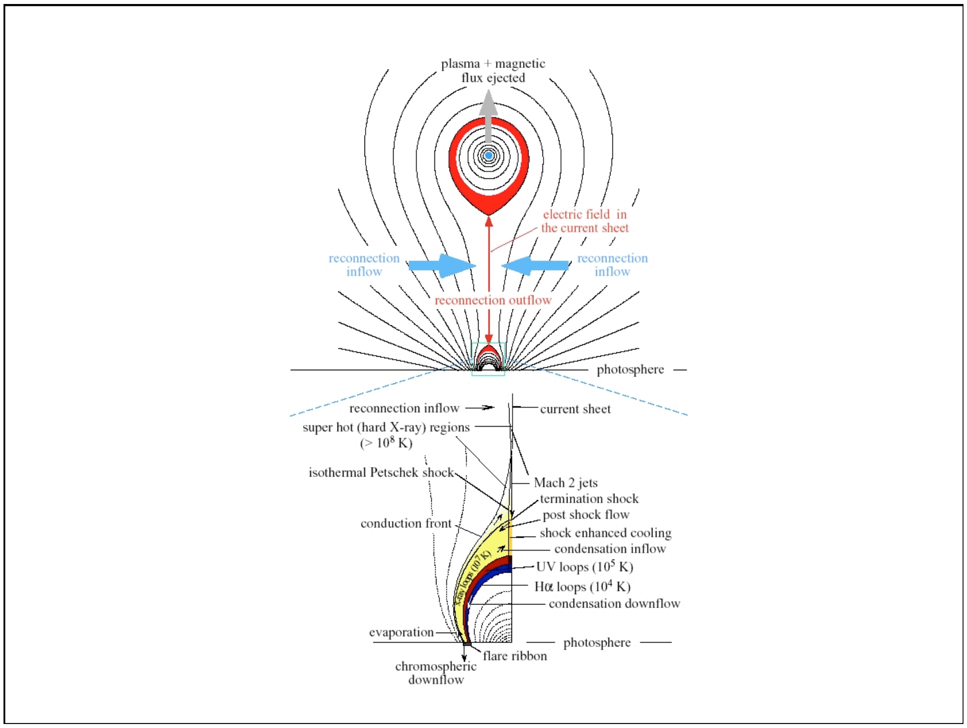

plasma + magnetic flux ejected
electric field in the current sheet
reconnection inflow
reconnection inflow
reconnection outflow
photosphere
reconnection inflow
current sheet
super hot (hard X-ray) regions (> 10^8 K)
isothermal Petschek shock
Mach 2 jets
termination shock
post shock flow
conduction front
shock enhanced cooling
condensation inflow
UV loops (10^5 K)
Hα loops (10^4 K)
condensation downflow
evaporation
photosphere
flare ribbon
chromospheric downflow

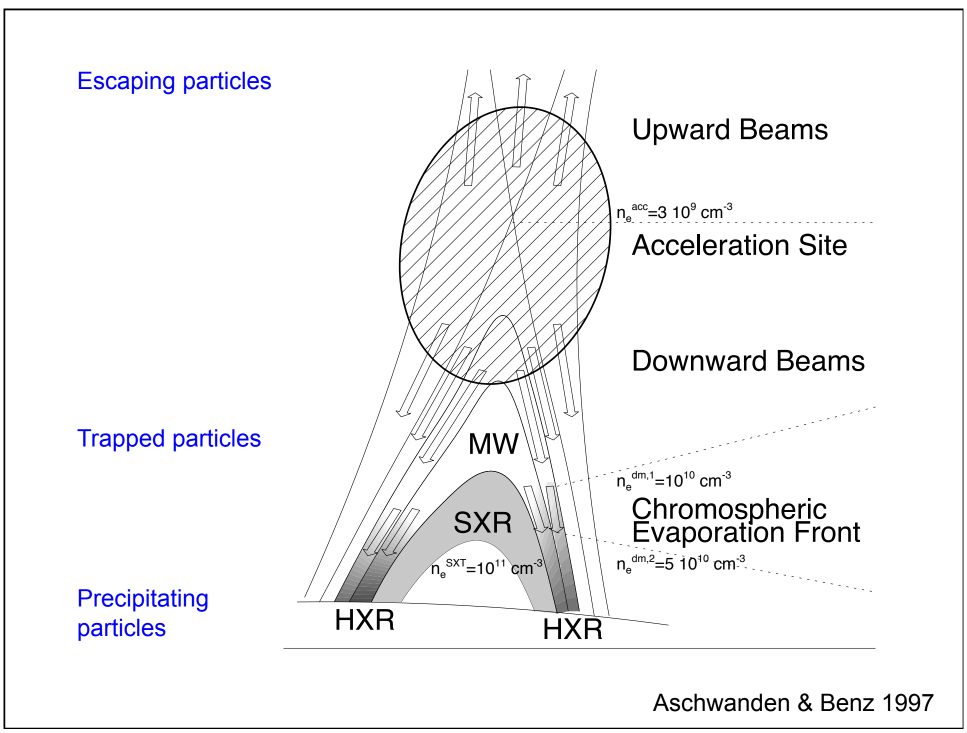

Escaping particles
Upward Beams
n_e^{acc}=3 10^9 cm^-3
Acceleration Site
Downward Beams
Trapped particles
MW
$n_e^{dm,1}$=10^10 cm^-3
Chromospheric Evaporation Front
SXR
n_e^{SXT}=10^11 cm^-3
$n_e^{dm,2}$=5 10^10 cm^-3
Precipitating particles
HXR
HXR
Aschwanden & Benz 1997

Lecture Plan

- Overview of the electromagnetic spectrum
- Preliminaries
- Emission Mechanisms
  - Radio wavelengths
    - ✓ Gyrosynchrotron radiation
    - ✓ Plasma radiation
  - HXR/Gamma-ray energies
    - ✓ Nonthermal bremsstralung
    - ✓ Compton & Inverse Compton scattering
    - ✓ Pion decay
    - ✓ Annihilation radiation
    - ✓ Neutron capture
    - ✓ Nuclear excitation
- Examples (time permitting …)

Preliminaries

Specific intensity (cf. diff'l intensity)

$$dE = \mathcal{I}_\nu \; dA \; dt \; d\Omega \; d\nu$$

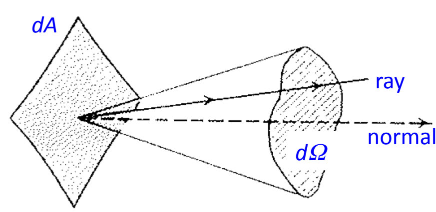

Flux density

$$F_\nu = \int \mathcal{I}_\nu \cos\theta \; d\Omega$$

Units

Specific intensity: ergs cm^{-2} s^{-1} Hz^{-1} sr^{-1}

Flux density*: ergs cm^{-2} s^{-1} Hz^{-1} (or ergs cm^{-2} s^{-1} keV^{-1} or counts cm^{-2} s^{-1} keV^{-1})

Total flux: ergs cm^{-2} s^{-1}

Fluence: ergs cm^{-2}

*1 Jansky (Jy) = 10^{-26} ergs cm^{-2} s^{-1} Hz^{-1}
1 solar flux unit (SFU) = 10^4 Jy

In the absence of emission, absorption, or scattering the specific intensity along a ray does not change. However, if emission and absorption occur, the radiative transfer equation is

$$\frac{d\mathcal{I}_\nu}{ds} = -\alpha_\nu \mathcal{I}_\nu + j_\nu$$

where α_ν is the absorption coefficient (units cm^{-1}) and j_ν is the emission coefficient (units ergs cm^{-3} s^{-1} sr^{-1} Hz^{-1}). Defining the optical depth $\tau_\nu = \alpha_\nu ds$ and the source function $S_\nu = j_\nu / \alpha_\nu$ the transfer equation can be rewritten

$$\frac{d\mathcal{I}_\nu}{d\tau_\nu} = -\mathcal{I}_\nu + S_\nu$$

For an isolated and homogeneous source the solution is simply

$$\mathcal{I}_\nu(\tau_\nu) = \mathcal{S}_\nu(1 - e^{-\tau_\nu})$$

When $\tau_\nu >> 1$, the source is said to be optically thick and $\mathcal{I}_\nu = \mathcal{S}_\nu$; when $\tau_\nu << 1$, the source is said to be optically thin and $\mathcal{I}_\nu \approx \tau_\nu \mathcal{S}_\nu$

For a system of matter and radiation in thermodynamic equilibrium it is characterized everywhere by a single temperature T and the differential density distribution is given by the Maxwell-Boltzmann distribution

$$n(E)dE = \left(\frac{2}{\pi}\right)^{1/2} \frac{N}{k_B T} \left(\frac{E}{k_B T}\right)^{1/2} \exp[-\frac{E}{k_B T}]dE$$

The specific intensity, referred to under these circumstances as blackbody radiation, is described by the Planck function

$$B_\nu(T) = \frac{2h\nu^3/c^2}{e^{h\nu/k_B T} - 1}$$

Note that at radio wavelengths we have $h\nu << k_B T$ and so

$$B_\nu(T) = I_\nu(T) \approx \frac{2\nu^2}{c^2} kT$$

a relationship known as the Rayleigh-Jeans Law.

Given the simplicity of the Planckian in the Rayleigh-Jeans regime, it is useful to can define the brightness temperature:

$$\mathcal{I}_\nu = \mathcal{B}_\nu(T_B) = \frac{2\nu^2}{c^2} kT_B$$

and the effective temperature:

$$\mathcal{S}_\nu = \frac{2\nu^2}{c^2} kT_{eff}$$

Note that the transfer equation can now be written:

$$\frac{dT_B}{d\tau_\nu} = -T_B + T_{eff}$$

with solutions $T_B = T_{eff} = T$ when the source is optically thick and $T_B = \tau_\nu T_{eff}$ when the source is optically thin.

Radiation from a Maxwellian particle distribution is referred to as thermal radiation whereas radiation from a non-Maxwellian particle distribution is referred to as nonthermal radiation.

Example of a nonthermal distribution:

$$n(E)dE = CNE^{-\delta}dE$$

$$C = (\delta - 1)E_C^{\delta - 1}$$

Lecture Plan

- Overview of the electromagnetic spectrum
- Preliminaries
- Emission Mechanisms
  - Radio wavelengths
    - ✓ Gyrosynchrotron radiation
    - ✓ Plasma radiation
  - HXR/Gamma-ray energies
    - ✓ Nonthermal bremsstrahlung
    - ✓ Compton & Inverse Compton scattering
    - ✓ Pion decay
    - ✓ Annihilation radiation
    - ✓ Neutron capture
    - ✓ Nuclear excitation
- Examples (time permitting …)

Radio Emission

- Thermal bremsstrahlung (e-p)
- Gyrosynchrotron radiation (e-B)
- Plasma radiation (w-w)

Larmor formulae: radiation from an accelerated charge

$$\frac{dP}{d\Omega} = \frac{q^2}{4\pi c^3}\mathbf{a}^2 \sin^2\theta \qquad P = \frac{2q^2}{3c^3}\mathbf{a}^2$$

Relativistic Larmor formulae

$$\frac{dP}{d\Omega} = \frac{q^2}{4\pi c^3}\frac{(a_\perp^2 + \gamma^2 a_\parallel^2)}{(1-\beta\cos\theta)^4}\sin^2\theta$$

$$P = \frac{2q^2}{3c^3}\gamma^4({a_\perp}^2 + \gamma^2 a_\parallel^2)$$

Cases relevant to radio and HXR/gamma-ray emission:

Acceleration experienced in the Coulomb field: bremsstrahlung
Acceleration experience in a magnetic field: gyromagnetic radiation

Electron-ion Bremsstrahlung

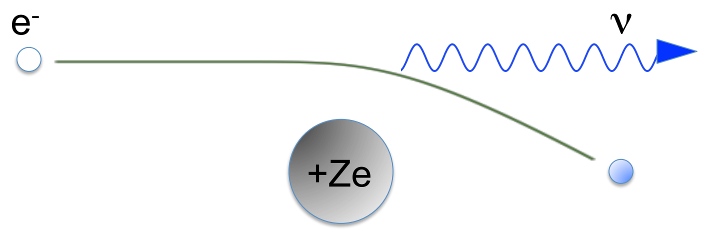

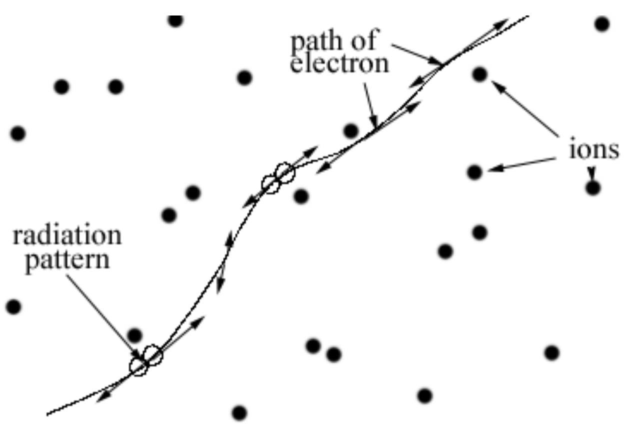

- At radio wavelengths, thermal bremsstrahlung or thermal free-free radiation is relevant to the quiet Sun, flares, and CMEs
- Nonthermal bremsstrahlung is relevant to HXR/gamma-ray bursts

Gyromagnetic radiation

$$\mathbf{a} = \frac{q}{mc}\mathbf{v} \times \mathbf{B}$$

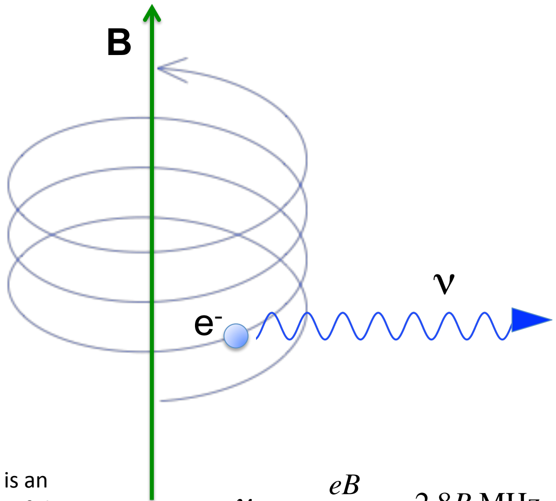

The electron gyrofrequency is an important natural frequency of the solar corona.

$$\nu_{Be} = \frac{eB}{2\pi m_e c} = 2.8B \text{ MHz}$$

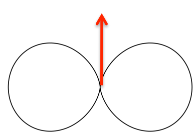

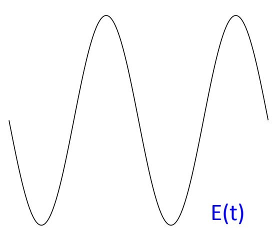

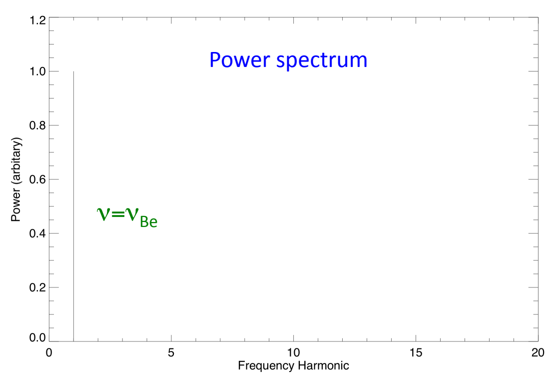

γ=1

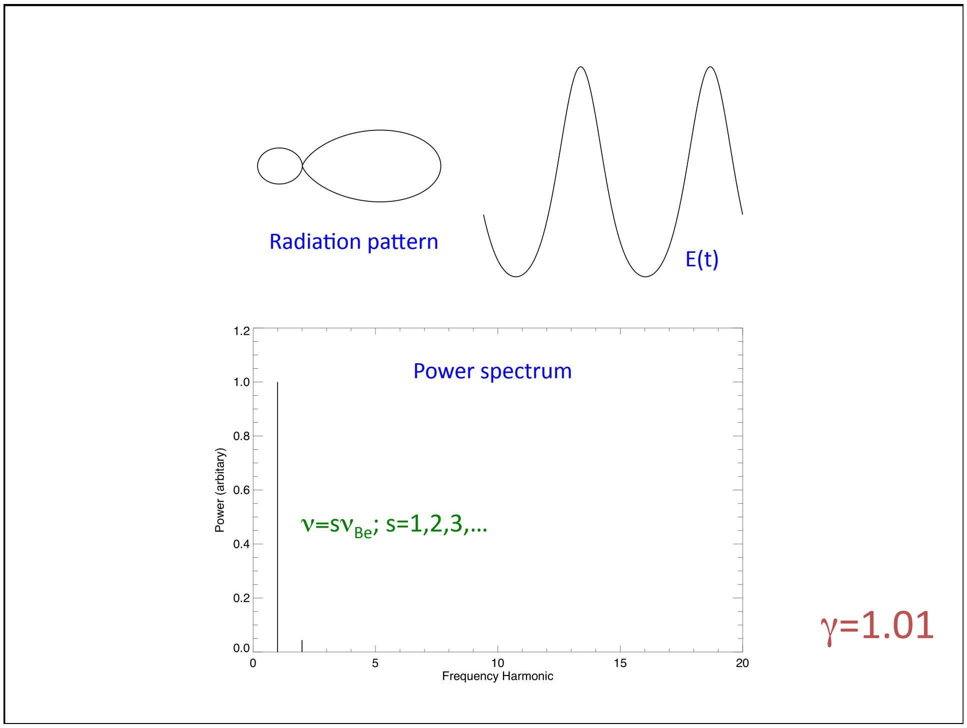
Radiation pattern
E(t)
Power spectrum
$\nu = s\nu_{Be}$; s=1,2,3,...
Power (arbitary)
Frequency Harmonic
γ=1.01

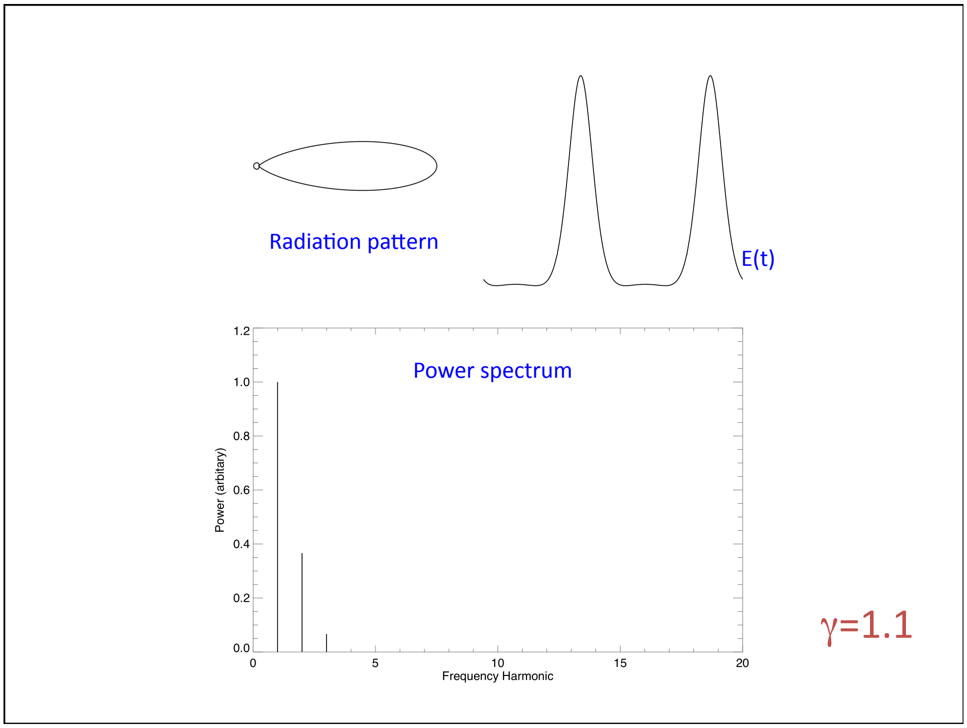
Radiation pattern
E(t)
Power spectrum
Power (arbitary)
Frequency Harmonic
γ=1.1

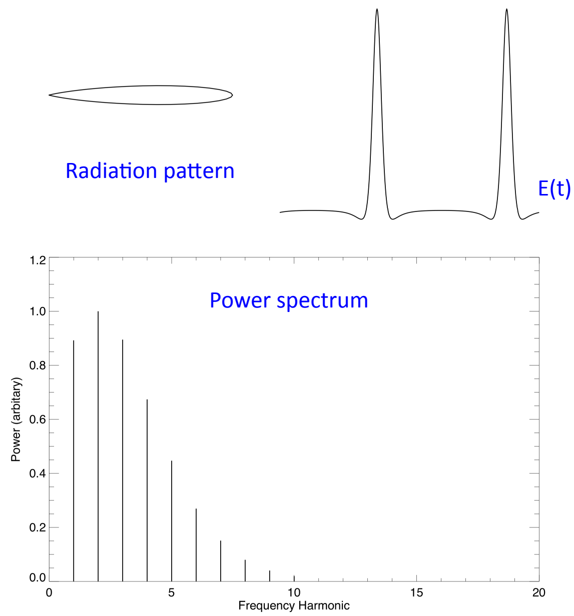

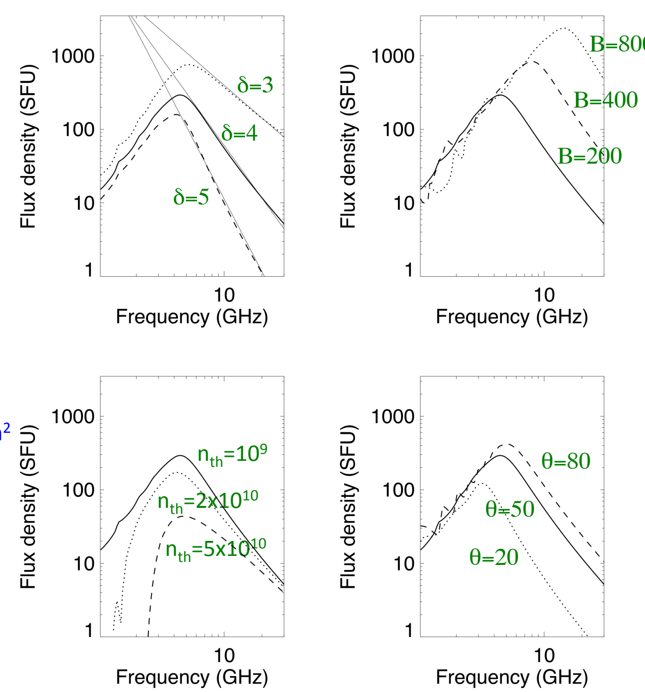

Reference spectrum

B=200 G

δ=4

E_c=100 keV

$n_{th}=10^9$ cm^{-3}

$n_{rl}=10^5$ cm^{-3}

A=3 x 10^{18} cm^2

D=10^9 cm

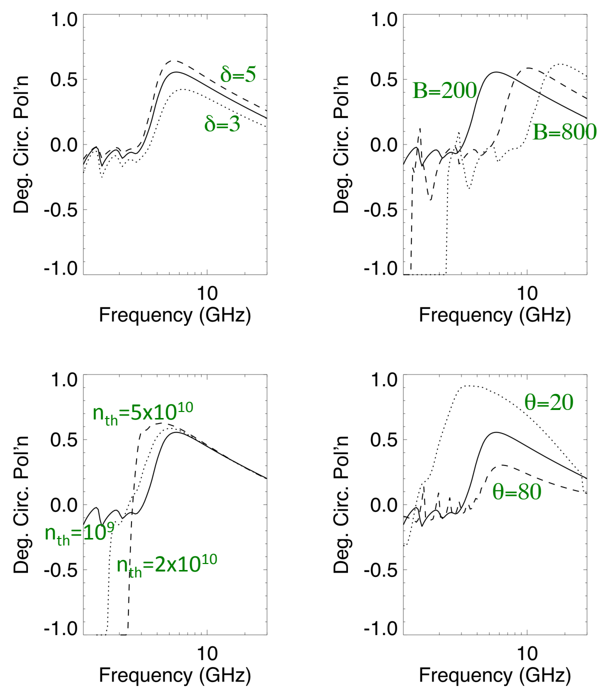

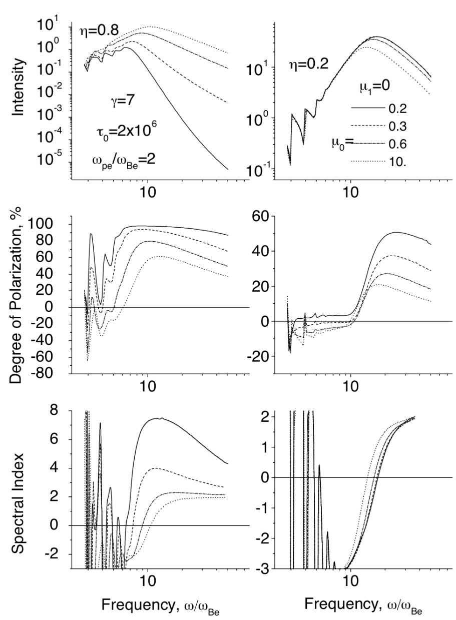

Anisotropic electron distributions

Affects spectrum and polarization properties of the emitted spectrum!

Unless properly accounted for, incorrect conclusions will be drawn.

Fleishman & Melnikov 2003

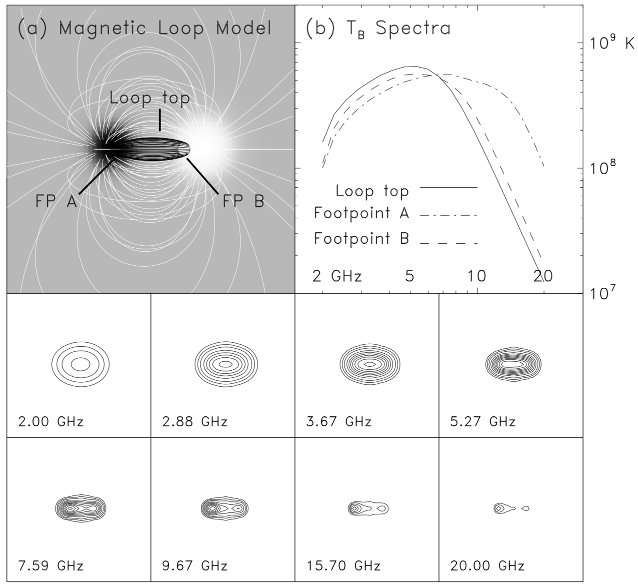

Bastian et al 1998

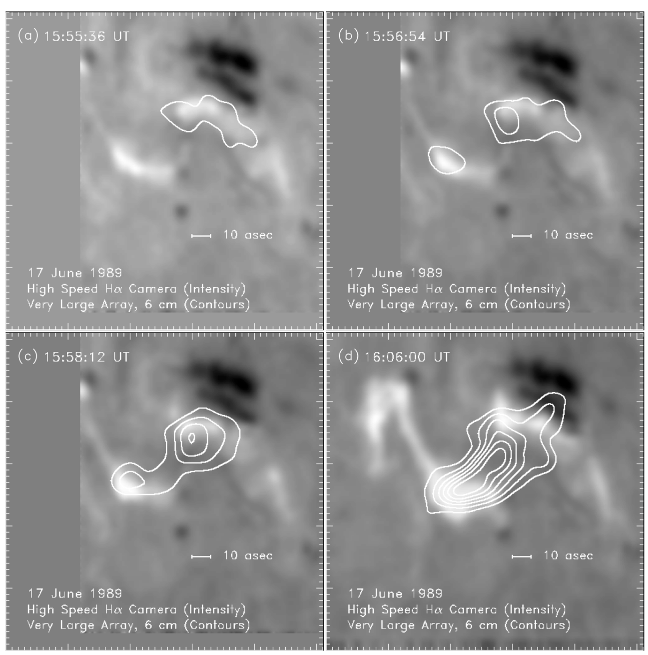

Bastian & Kiplinger 1991

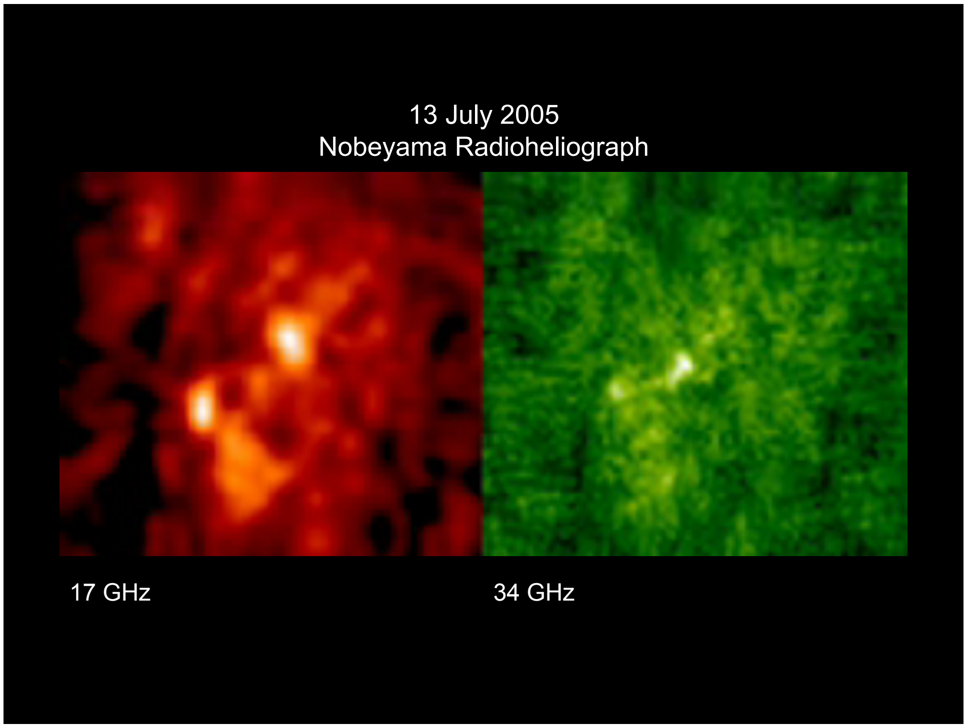

Plasma radiation

Plasma waves, also called Langmuir waves, are electrostatic oscillations. The oscillation frequency is the electron plasma frequency, the second natural frequency in the solar atmosphere relevant to radio emission:

$$\nu_{pe} = \omega_{pe}/2\pi = \sqrt{e^2 n_e/\pi m_e} = 9 n_e^{1/2} \text{ kHz}$$

Dispersion relation for electromagnetic (radio) waves:

$$\omega^2 = k^2 c^2$$
in vacuo

$$\omega^2 = k^2 c^2 + \omega_{pe}^2$$
in a plasma

For Langmuir waves:

$$\omega^2 = \omega_{pe}^2$$
"cold plasma"

$$\omega^2 = \omega_{pe}^2 + 3k^2 v_{th}^2$$
warm plasma

Langmuir waves are excited by anisotropies in the electron distribution function that can arise from electron beams, loss cones, or other distributions.

Plasma radiation arises when (longitudinal) Langmuir waves are converted to (transverse) electromagnetic waves via wave-wave interactions.

Plasma radiation at $\nu=\nu_{pe}$ (fundamental) is produced when Langmuir waves interact with ion sound waves:

$$L + s \rightarrow T$$

Plasma radiation at $\nu=2\nu_{pe}$ (harmonic) is produced when two Langmuir waves coalesce:

$$L + L' \longrightarrow T$$

Such Langmuir waves must essentially collide head-on in order to conserve momentum. Note that an important ancillary reaction is the decay of Langmuir waves into a secondary Langmuir wave and an ion sound wave.

$$L \longrightarrow L' + s$$

Two important examples of plasma radiation phenomena relevant to heliophysics:

- Type II radio burst: plasma radiation associated with a coronal or IP shock
- Type III radio bursts: plasma radiation associated with an electron beam

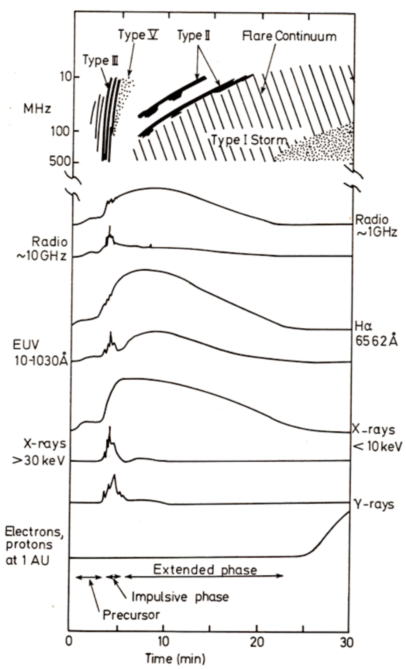

Dulk 1985

GB/SRBS

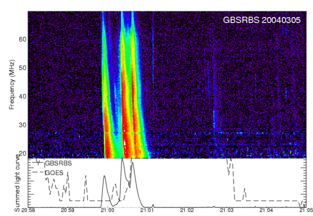

type III

type III + type II

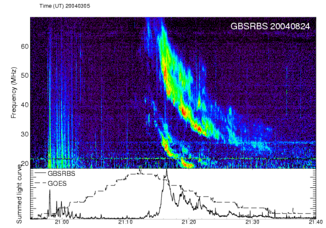

type II + type IV + fadeout

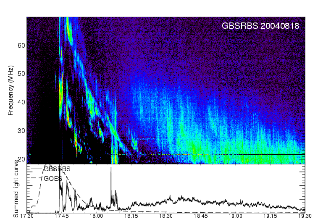

Lecture Plan

- Overview of the electromagnetic spectrum
- Preliminaries
- Emission Mechanisms
  - Radio wavelengths
    - ✓ Gyrosynchrotron radiation
    - ✓ Plasma radiation
  - HXR/Gamma-ray energies
    - ✓ Nonthermal bremsstrahlung
    - ✓ Compton & Inverse Compton scattering
    - ✓ Pion decay
    - ✓ Annihilation radiation
    - ✓ Neutron capture
    - ✓ Nuclear excitation
- Examples (time permitting …)

Hard X-ray & Gamma-ray Radiation

- Nonthermal bremsstrahlung
- Compton & inverse Compton scattering
- Pion decay
- Positron annihilation
- Neutron capture
- Nuclear excitation

Nonthermal bremsstrahlung radiation

A HXR photon is emitted when an energetic electron scatters off the Coulomb field of a proton (or other ion).

Consider an energetic electron in a uniform, fully ionized hydrogen plasma with a proton density n_p. The photon production rate is then just $n_p\,\sigma_\varepsilon(E)\,v(E)$. Consider a distribution of energetic electrons $N(E)\,dE$. Then the total photon rate produced by the (optically thin) source volume V is

$$n_p V \int_\epsilon^\infty \sigma_\epsilon(E) v(E) N(E) dE$$

and the photon count rate at Earth (R = 1 AU) is then

$$S(\epsilon) = \frac{n_p V}{4\pi R^2} \int_\epsilon^\infty \sigma_\epsilon(E) v(E) N(E) dE$$

in units of photons $cm^{-2}\ s^{-1}$ per unit energy.

This is referred to as "thin target" emission because the time scale for Coulomb losses by the energetic electrons is much greater than any other time scale relevant to the flare.

The photon cross section used for HXR emission is the *Bethe-Heitler* cross section, valid for non-relativistic to weakly relativistic electrons:

$$\sigma_\epsilon(E) = \frac{8}{3}\alpha r_\circ^2 \frac{m_e c^2}{\epsilon E} \log \frac{1+\sqrt{1-\epsilon/E}}{1-\sqrt{1-\epsilon/E}}$$
$$= \frac{16}{3}\alpha r_\circ^2 \frac{m_e c^2}{\epsilon E} \log\left(\sqrt{E/\epsilon} + \sqrt{1 - E/\epsilon}\right)$$

Rewriting the photon count rate,

$$S(\epsilon) = \frac{2\beta}{\epsilon} \int_\epsilon^\infty \frac{N(E)}{\sqrt{E}} \log\left(\sqrt{E/\epsilon} + \sqrt{1 - E/\epsilon}\right) dE$$

where $$\beta = \frac{2}{3}\alpha n_\circ \left(\frac{r_\circ}{R}\right)^2 m_e c^2 \sqrt{\frac{2}{m_e}}$$

Suppose the energetic electron distribution function is a power law:

$$N(E) = KE^{-\delta}$$

With a change of variables from E to E/ε we then have

$$KE^{-\delta} = K\epsilon^{-\delta}u^{-\delta}, \qquad u = E/\epsilon$$

and the photon count at 1 AU is recast as

$$S(\epsilon) = 2\beta K\epsilon^{-(\delta+1/2)}\int_1^{\infty} u^{-(\delta+1/2)}\log\Big(\sqrt{u}+\sqrt{1-u}\Big)du$$

$$S(\epsilon) \propto \epsilon^{-(\delta+1/2)}$$

This result was obtained by Brown (1971), although instead it was formulated in terms of the observed photon spectrum, taken to be a power law,

$$S(\epsilon) = K_2\epsilon^{-\gamma}$$

from which $N(E)$ was inferred through inversion: $N(E) \propto E^{-(\gamma-1/2)}$

Now consider the case where we have a continuous injection of fast electrons into the source volume where they suffer energy losses via collisions on free (and bound) electrons and are brought to a stop.

For a fully ionized plasma we have

$$\frac{dE}{dt} = -n_p v(E)E\sigma_{ee}(E)$$

where $\sigma_{ee}(E) = \frac{2\pi e^4}{E^2}\Lambda_{ee}(E); \qquad \Lambda_{ee}(E) = log\Big(\frac{E}{e^2}b_{max}\Big)$

An electron injected with an energy E_o can radiate photons with energy ε via bremsstrahlung until the electron's energy has fallen below ε. It's photon production rate is then given by:

$$\nu(\epsilon, E_\circ) = \int_{t(E=E_\circ)}^{t(E=\epsilon)}\sigma_\epsilon(E)n_p v(E)dt = \frac{1}{C}\int_\epsilon^{E_\circ} E\sigma_\epsilon(E)dE$$

where $C = 2\pi e^4\Lambda_e e(E)$

Now if a distribution of $F(E_o)$ electrons per unit energy are injected into the source volume each second, the total photon emission rate is

$$\nu_{tot}(\epsilon) = \int_{\epsilon}^{\infty} F(E_\circ)\nu(\epsilon, E_\circ)dE_\circ$$

and the photon flux per unit energy at Earth is then

$$S(\epsilon) = \frac{2\beta}{\epsilon}\frac{1}{Cn_\circ}\sqrt{\frac{m_e}{2}}\int_{\epsilon}^{\infty} F(E_\circ)\left[\int_{\epsilon}^{E_\circ}\log\left(\sqrt{E/\epsilon}+\sqrt{1-E/\epsilon}\right)dE\right]dE_\circ$$

Exchanging the order of integration, this can be rewritten

$$= \frac{2\beta}{\epsilon}\frac{1}{Cn_\circ}\sqrt{\frac{m_e}{2}}\int_{\epsilon}^{\infty}\phi(E)\log\left(\sqrt{E/\epsilon}+\sqrt{1-E/\epsilon}\right)dE$$

where $\phi(E) = \int_{E}^{\infty} F(E_\circ)dE_\circ$

As before, we assume a power-law distribution of electrons is injected into the source. Then we have

$$\phi(E) = \frac{K_1}{\delta - 1}E^{-(\delta-1)} = K_1\epsilon^{-(\delta-1)}u^{-(\delta-1)}$$

With the same change of variables as before we can then write

$$S(\epsilon) = \frac{2\beta K_1}{Cn_\circ}\sqrt{\frac{m_e}{2}}\epsilon^{-(\delta-1)}\int_{1}^{\infty} u^{-(\delta-1)}\log\left(\sqrt{u}+\sqrt{1-u}\right)du$$

and it's seen for "thick target" emission,

$$S(\epsilon) \propto \epsilon^{-(\delta-1)}$$

or, inverting a power-law photon spectrum,

$$F(E) \propto E^{-(\gamma+1)}$$

In order to directly compare with the thin target case we note that

$$F(E) \sim v(E)N(E) \propto E^{1/2}N(E) \propto E^{-(\gamma-1)}$$

The inferred index of the injection spectrum to be flatter by 2 for the thin target case ($\gamma-1$) than inferred for the thick target case ($\gamma+1$).

Alternatively, for a given electron injection spectrum with an index δ, the resulting photon spectral index is steeper by 2 for a thin target source ($\delta+1$) than it is for a thick target source ($\delta-1$).

Thin-target emission

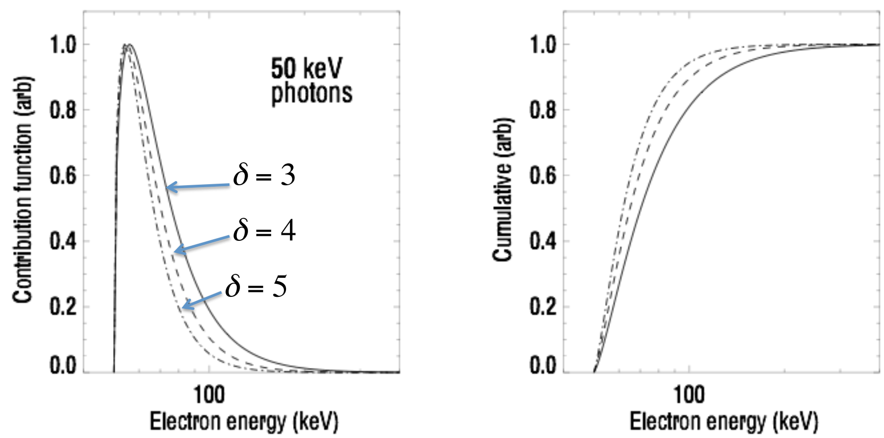

Thick-target emission

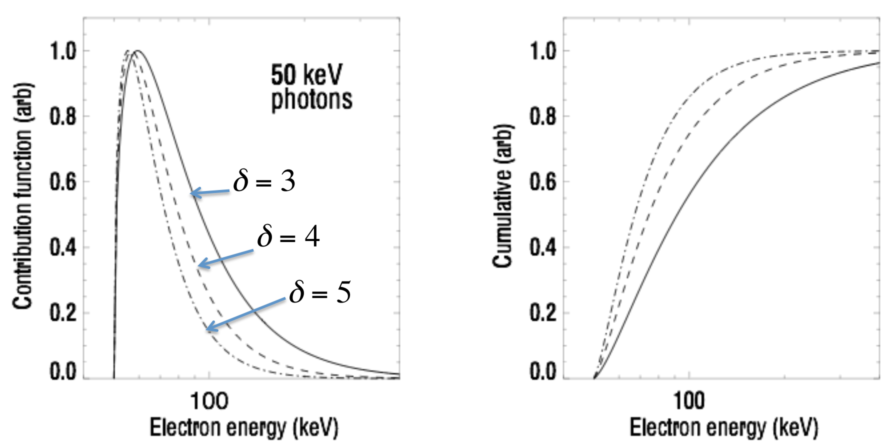

Other bremsstrahlung contributions

At higher (relativistic) energies, corrections to the electron-proton photon cross section must be included. Moreover, additional contributions to the bremsstrahlung photon spectrum may need to be included. These are:

- Electron-electron bremsstrahlung (e.g., Haug 1975; Kontar 2007)
- Positron-electron bremsstrahlung (e.g., Haug 1985)

Another point: in principle, protons accelerated in a flare also stream down to the chromosphere and photosphere where they should produce bremsstrahlung by scattering on ambient electrons. That is,

- Proton-electron bremsstrahlung (Emslie & Brown 1985; Haug 2003)

This "inverse bremsstrahlung" is not widely believed to be significant, however.

Compton scattering

The scattering of photons on electrons, or vice versa, appears in several guises:

- Thomson scattering: low energy photons elastically scatter off low energy electrons – e.g., the white light corona
- Compton scattering: energetic photons scatter off low energy electrons – e.g., HXR albedo patch

HXR photons of 10-100 keV Compton backscatter from the low solar atmosphere. The Compton scattering cross section has a broad maximum at 30-40 keV. The reflectivity can approach unity.

It is therefore important to take into account the HXR albedo flux when interpreting HXR spectra (at least those now available from RHESSI)!

Complications: the albedo patch depends on the relative geometry of the source region to the atmosphere, the aspect angle, and the polarization of the HXR photons (e.g., Kontar et al. 2006, Kasparova et al. 2007)

48

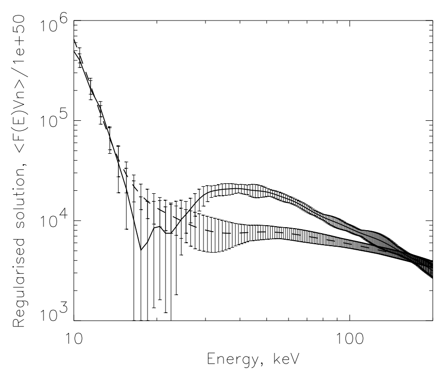

Fig. 8. Inverted mean electron flux of the August 20, 2002 solar flare for the time interval 08:25:20- 08:25:40 UT. The dash line shows the spectra with albedo correction. The confidence intervals represent the range of solutions found by allowing the incident photon spectrum to range randomly within the estimated (instrument + shot noise) errors.

Kontar et al 2006

Inverse Compton scattering

- Inverse Compton scattering: soft photons scatter off of energetic electrons – e.g., coronal HXR sources

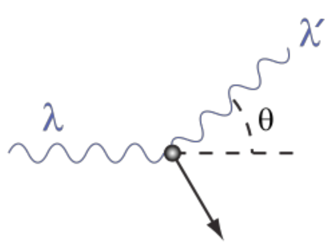

$$\lambda' - \lambda = \frac{h}{m_e c}(1 - \cos\theta)$$

$$\varepsilon' = \frac{\varepsilon}{1 + (\varepsilon / m_e c^2)(1 - \cos\theta)}$$

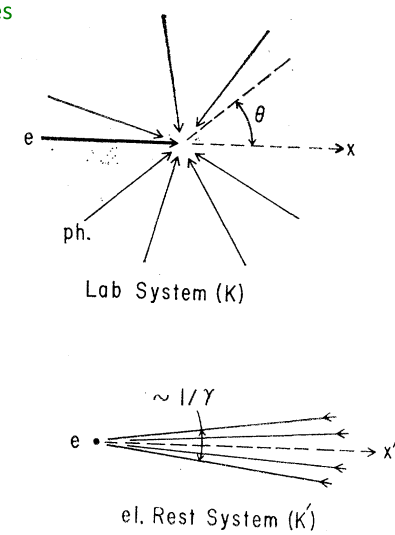

50

Relativistic electron

Rest frame

$$\varepsilon_r = \gamma\varepsilon(1-\cos\theta)$$

$$\varepsilon_r' = \frac{\varepsilon_r}{1+\left(\varepsilon/m_e c^2\right)\left(1-\cos\theta_r\right)}$$

Lab frame

$$\varepsilon_l' = \gamma\varepsilon_r'\left(1-\beta\cos\theta_r\right)$$

$$\varepsilon_l'(\max) \approx 2\gamma\varepsilon_r'$$

Thomson regime

$$\varepsilon << m_e c^2$$

$$\varepsilon' \approx \varepsilon$$

$$\varepsilon_l'(\max) \approx 2\gamma\varepsilon_r'(\max) \approx 4\gamma^2\varepsilon$$

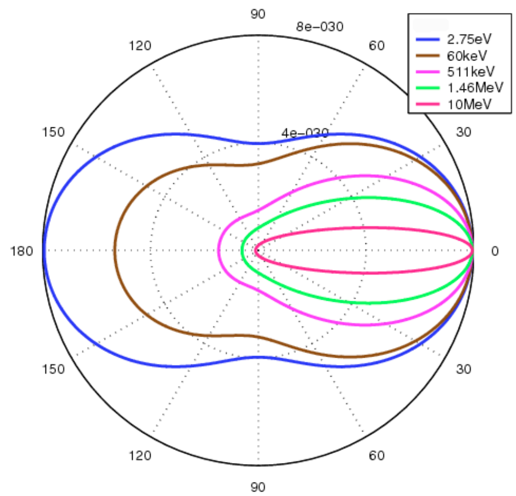

51

Coronal HXR sources

MacKinnon & Mallik (2010) consider the case wherein photospheric photons (2 eV) are up-scattered by a power-law distribution of ultra-relativistic flare electrons or positrons.

They include consideration of the anisotropic photon field and varying aspect angle.

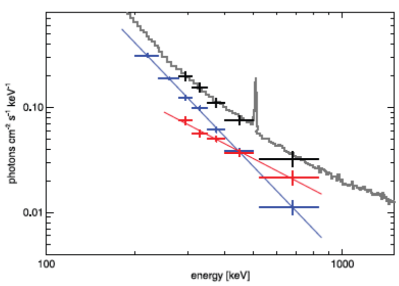

They find that if ultra-relativistic electrons are present – as was the case for the 2005 Jan 20 flare – then the IC mechanism can rather easily account for the observed HXR spectrum.

Caveat: the ambient plasma density must be low ($<10^{10}$ cm^{-3}).

52

Gamma-ray Emission

Gamma-rays are produced by the interaction of energetic protons, alpha particles, and heavy nuclei with the ambient chromospheric and photospheric plasma.

Consider a particle species *j* that has been accelerated to a high energy and is incident on an ambient particle species i. The interaction rate can be written as

$$\nu_{ij} = n_i \int_0^\infty N_j(E)\sigma_{ij}(E)v(E)dE$$

We again formulate the problem in terms of thin- or thick-target emission. Thin target processes are relevant to particles that escape into the IPM. Here, we discuss thick-target processes. The yield of particles (e.g., neutrons, positrons, pions) from a particular interaction in the thick target case is given by (Ramaty et al 1986):

$$Q = \frac{1}{m_p}\sum_{ij}\frac{n_i}{n_H}\int_0^\infty \bar{N}_j(E)dE\int_0^\infty \frac{\sigma_{ij}(E')}{(dE'/dx)_j}dE'$$

Or, reversing the order of integration,

$$Q = \frac{1}{m_p}\sum_{ij}\frac{n_i}{n_H}\int_0^\infty \frac{\sigma_{ij}(E)}{(dE/dx)_j}dE\int_E^\infty \bar{N}_j(E')dE'$$

In our treatment of HXR bremsstrahlung we specified the dominant energy loss term (collisions with electrons) as a function of time. Here, the energy loss term(s) are left unspecified and are expressed as a function of range – depth into the source. Since energy loss by protons and ions is dominated by losses on H and He,

$$\left(\frac{dE}{dx}\right)_j \approx \left(\frac{dE}{dx}\right)_{j,H}\left[1 + \frac{n_{He}}{n_H}\frac{m_{He}}{m_p}\frac{(dE/dx)_{j,He}}{(dE/dx)_{j,H}}\right]$$

The terms in square brackets is approximately 1.13, and is nearly independent of energy.

$$\left(\frac{dE}{dx}\right)_{j,H} \approx 630\left(\frac{Z_{eff}^{\,2}}{A}\right)_j E^{-0.8} \qquad Z_{eff} = Z[1-\exp(-\beta/\alpha Z^{2/3})]$$

Again, the detailed physics is embodied in $\sigma_{ij}(E)$.

Pion decay

There are three types of π−mesons, or pions: π^o, π^+, and π^-. Neutral pions have a rest mass of about 135 MeV whereas the charged pions have a rest mass of about 140 MeV. The threshold energy for pion production is therefore ~300 MeV nuc^{-1}.

An example of an interaction that produces pions is proton-proton collisions:

$$p + p \longrightarrow \pi^+ + {}^2H$$

In the case of neutral pions, most (99%) decay directly into two photons. In the case of charged pions, they first decay to muons, then electrons and positrons.

$\pi^o \longrightarrow 2\gamma$ (each photon ~67 MeV, strongly Doppler broadened)

$$\pi^+ \longrightarrow \mu^+ + \nu_\mu \longrightarrow e^+ + \nu_e + \overline{\nu}_\mu$$
$$\pi^- \longrightarrow \mu^- + \overline{\nu}_\mu \longrightarrow e^- + \overline{\nu}_e + \nu_\mu$$

Secondary electrons → bremsstrahlung continuum
Secondary positrons → bremsstrahlung plus annihilation radiation

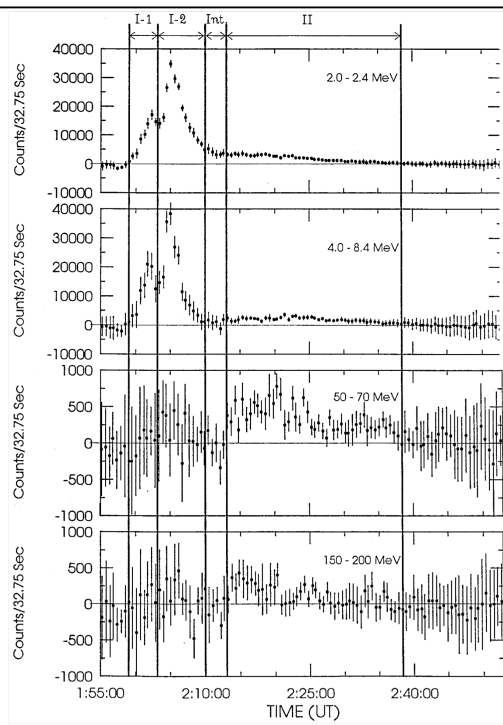

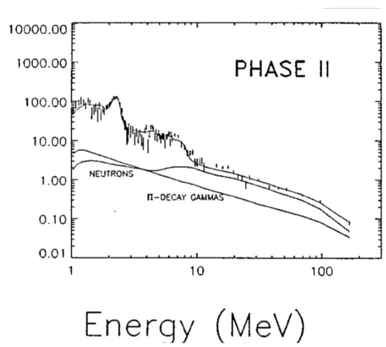

X12 flare of 11 Jun 1991
CGRO/EGRET

Dunphy et al 1999

Positron annihilation

Positrons are produced by two types of processes:

- π^+ decay (thresholds of 100s of MeV)
- β-decay of radioactive isotopes of C, N, and O (thresholds of 1-10s MeV)

Positrons are “born” relativistic. They initially lose energy to collisions with electrons and through ionization of neutrals until they have slowed sufficiently to:

1. annihilate on electrons, producing two photons, each 511 keV, OR
2. become bound to an ambient electron, forming positronium (Ps)

The subsequent decay of Ps depend on whether it is formed as spin-0 para-positronium (singlet state ^{1}Ps) or spin-1 orthopositronium (triplet state ^{3}Ps), the singlet state forming ¼ of the time, the latter forming ¾ of the time. The singlet state decays into two photons, each 511 keV. The triplet state decays into three photons, each with $\varepsilon < 511$ keV.

Direct annihilation of positrons and ^{1}Ps decay produce the 511 keV annihilation line; ^{3}Ps produces a continuum contribution below 511 keV.

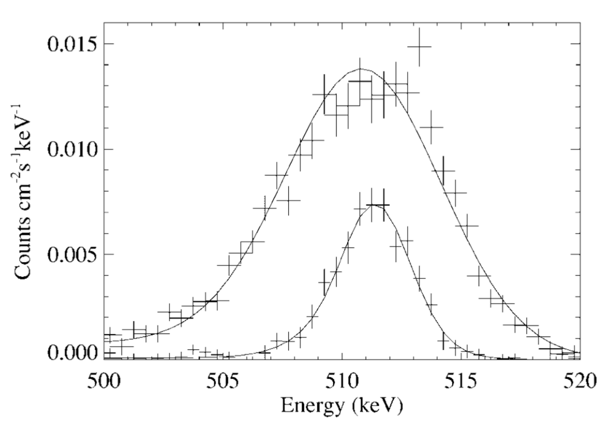

Fig. 3.—Count spectra of the solar 511 keV annihilation line (instrumentally broadened) derived by subtracting bremsstrahlung and nuclear contributions during the October 28 flare when the solar line was broad (11:06–11:16 UT) and narrow (11:18–11:30 UT). The solid curve is the best-fitting model that includes a Gaussian line and positronium continuum.

Share et al 2004

Nuclear de-excitation lines

Ambient heavy nuclei of C, N, O, as well as Ne, Mg, Al, Si, S, Ca, and Fe can be excited when bombarded by energetic protons and alpha particles.

Spallation and fusion (e.g., $\alpha-\alpha$) reactions also yield excited nuclear states.

Gamma-ray line radiation is produced when they de-excite. The line width – typically 10-100 keV – is determined by the recoil velocity of the nucleus in question.

- Strong lines of ^{12}C, ^{15}N and ^{16}O appear between 4-7 MeV
- Lines of the $\alpha-\alpha$, ^{20}Ne, ^{24}Mg, ^{26}Si, and ^{56}Fe reactions are seen <3 MeV
- Multitudes of weak narrow lines from nuclei heavier than O also contribute

In the inverse process energetic nuclei of C, N, O, and other heavies can bombard the ambient protons and helium, are excited and then de-excite, again emitting line radiation. However, in this case, the relevant nuclei are moving at high speeds and the emitted line radiation is significantly Doppler broadened which, combined with weak narrow lines forms a pseudo-continuum.

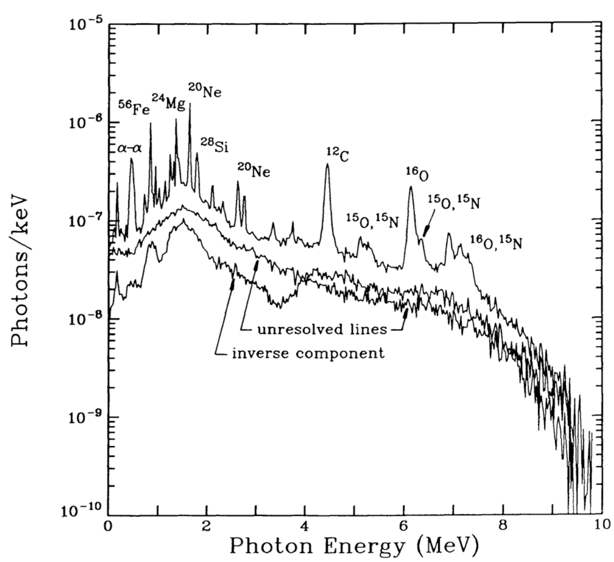

FIG. 1.—Theoretical solar flare nuclear de-excitation gamma-ray spectrum

Murphy et al 1990

Neutron capture line

A large number of processes can yield fast neutrons: proton-proton, proton-alpha, alpha-proton, alpha-alpha, as well as protons and alphas on heavy nuclei – e.g., $^{13}C(\alpha,n)^{16}O$ – and the inverse reactions. The threshold energy for these processes ranges from ~1 MeV nuc^{-1} (heavies) to 100s of MeV nuc^{-1} (proton-proton).

There are four possible fates for neutrons so produced:

1. They escape from the Sun
2. They decay: $n \longrightarrow p + e^- + \nu_e$ (photons only emitted via secondary electrons)
3. They charge exchange with ^3He, producing tritium: $^3He(n,p)^3H$ (no photon emitted)
4. They are captured onto H, producing deuterium: $^1H(n,p)^2H$ (photon emitted at 2.223 MeV)

Since the cross section for elastic scattering is much larger than that for either charge exchange or capture, neutrons thermalize before either (3) or (4) occurs, leading to a time delay of 10s to 100s of seconds before the 2.223 MeV line appears.

RHESSI observation of X4.8 flare of 23 July 2002

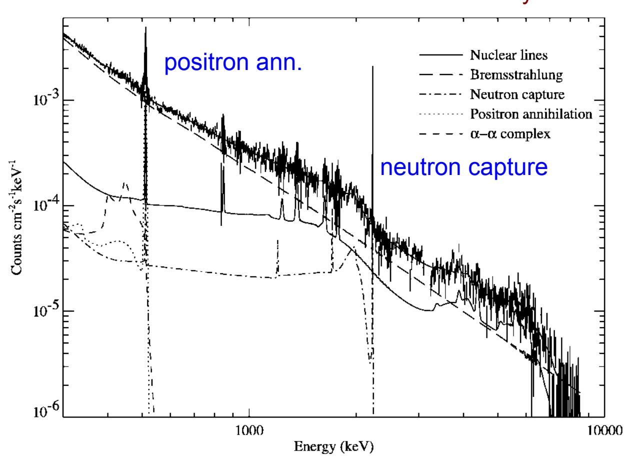

FIG. 3.—*RHESSI* γ-ray count spectrum from 0.3 to 10 MeV, integrated over the interval 0027:20–0043:20 UT. The lines show the different components of the model used to fit the spectrum.

Lin et al 2003

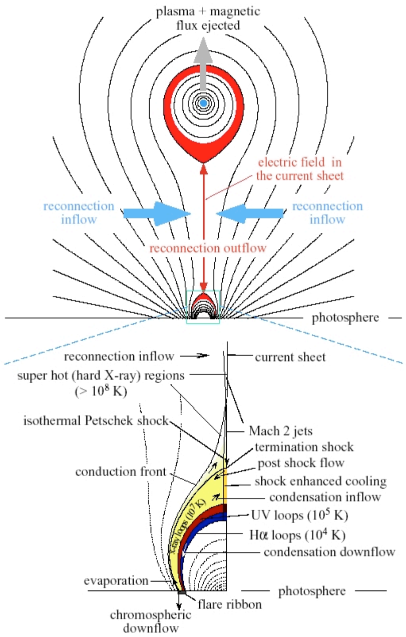

plasma + magnetic flux ejected
electric field in the current sheet
reconnection inflow
reconnection inflow
reconnection outflow
photosphere
reconnection inflow
current sheet
super hot (hard X-ray) regions (> 10^8 K)
isothermal Petschek shock
Mach 2 jets
termination shock
post shock flow
conduction front
shock enhanced cooling
condensation inflow
UV loops (10^5 K)
Hα loops (10^4 K)
condensation downflow
evaporation
photosphere
flare ribbon
chromospheric downflow

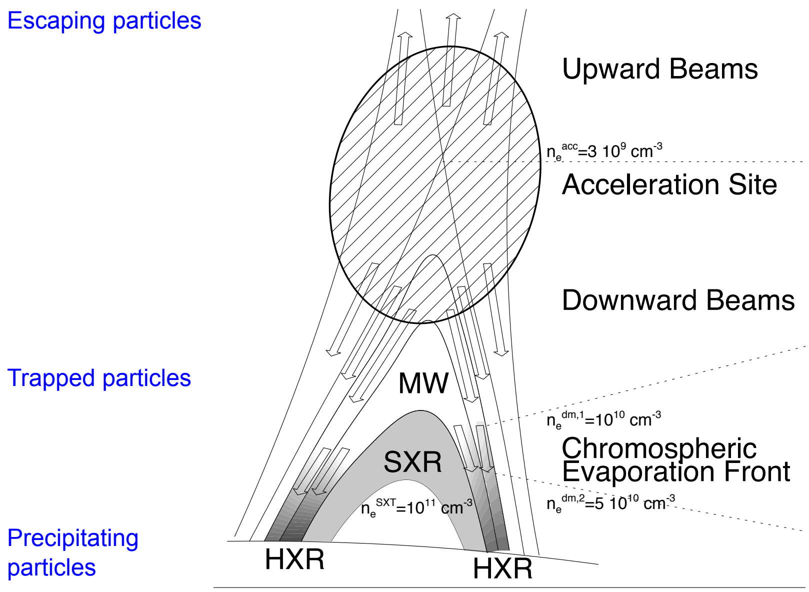

Aschwanden & Benz 1997

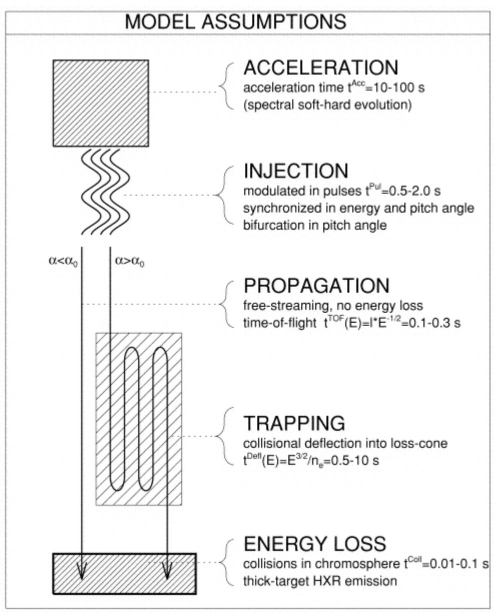

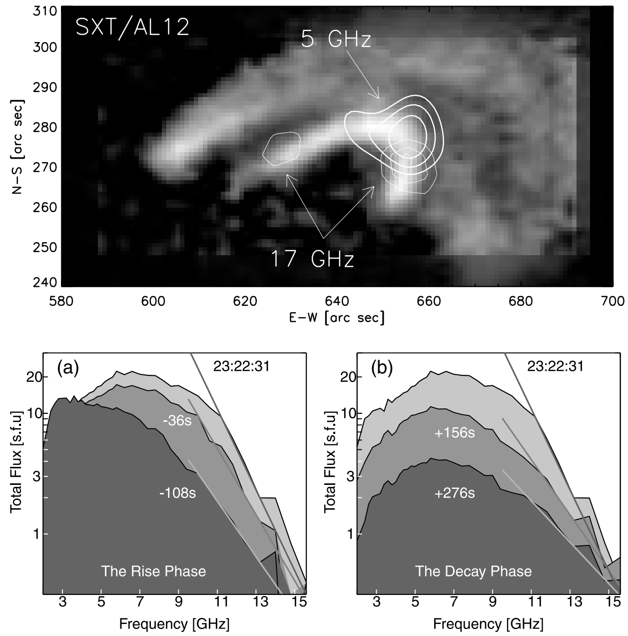

Lee & Gary 2000

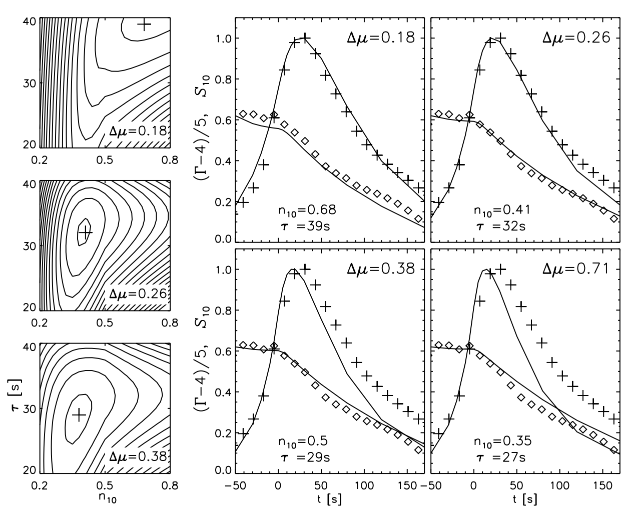

$$P_\gamma(\mu) = \frac{1}{\sqrt{\pi}\Delta\mu}\exp\left[-\frac{(\mu-\mu_o)^2}{\Delta\mu^2}\right]$$

$\mu = \cos\alpha$

$\alpha =$ pitch angle

- Mirroring
- Pitch-angle scattering
- Energy losses
- Anisotropy

Forward fitting via χ^2-minimization scheme shows electrons beamed perpendicular to B field

Lee & Gary 2000

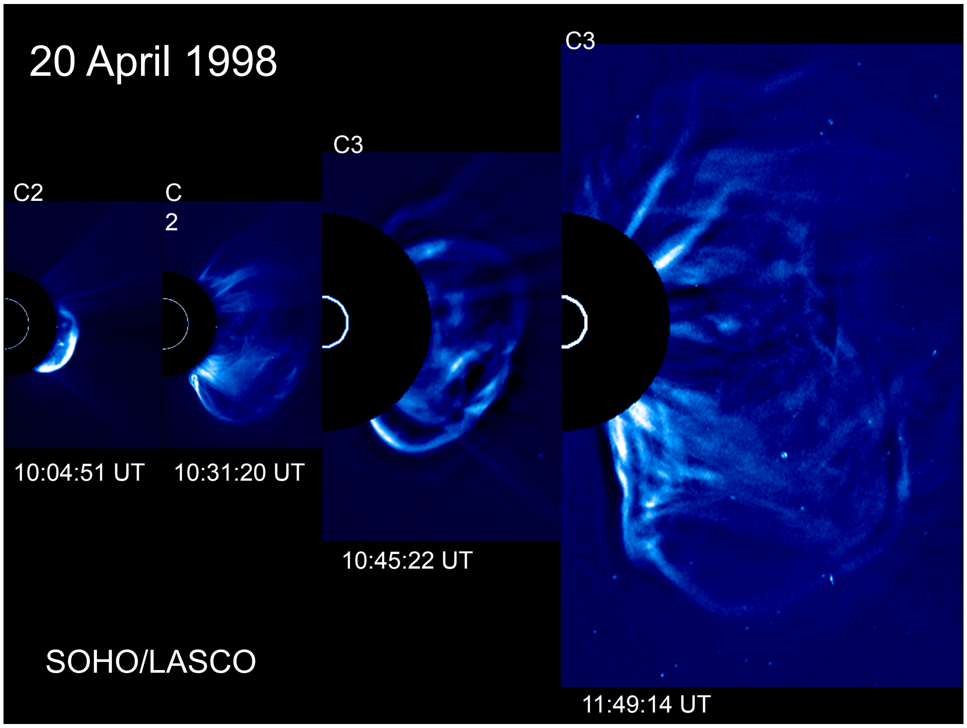
20 April 1998
C2
C
2
C3
C3
10:04:51 UT
10:31:20 UT
10:45:22 UT
11:49:14 UT
SOHO/LASCO

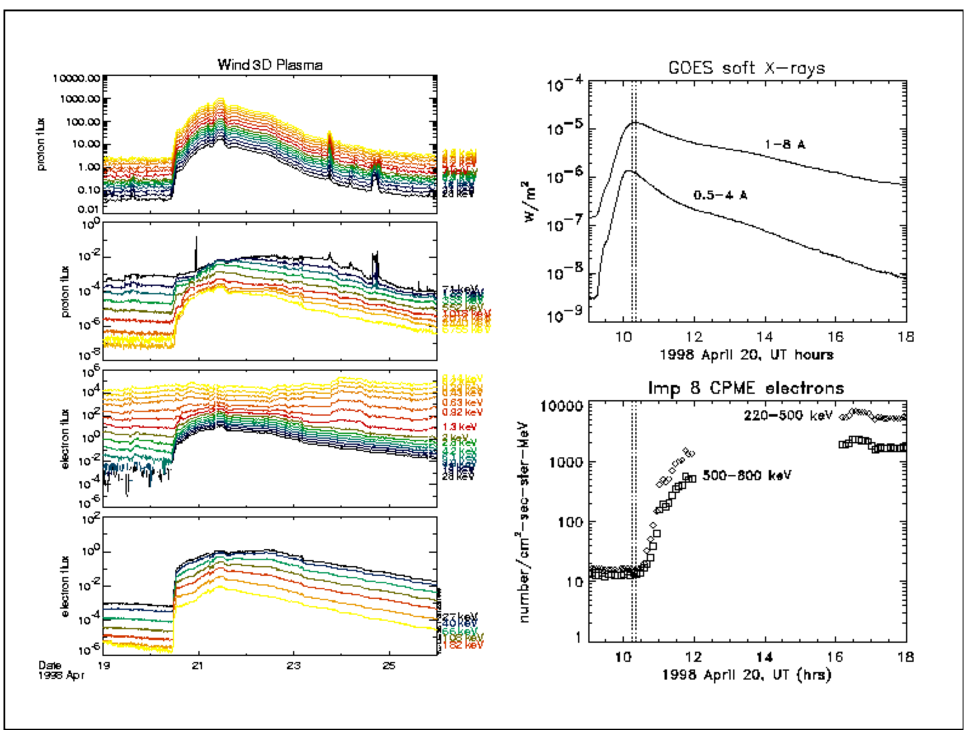
Wind 3D Plasma
proton flux
electron flux
Date
1998 Apr
GOES soft X-rays
1-8 A
0.5-4 A
W/m²
1998 April 20, UT hours
Imp 8 CPME electrons
220-500 keV
500-800 keV
number/cm²-sec-ster-MeV
1998 April 20, UT (hrs)

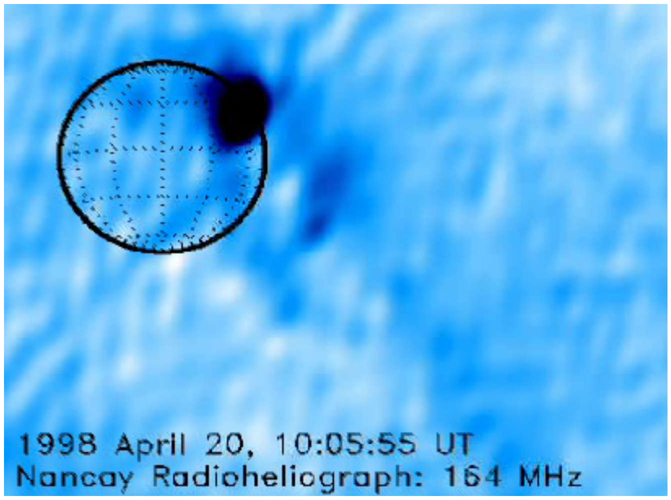

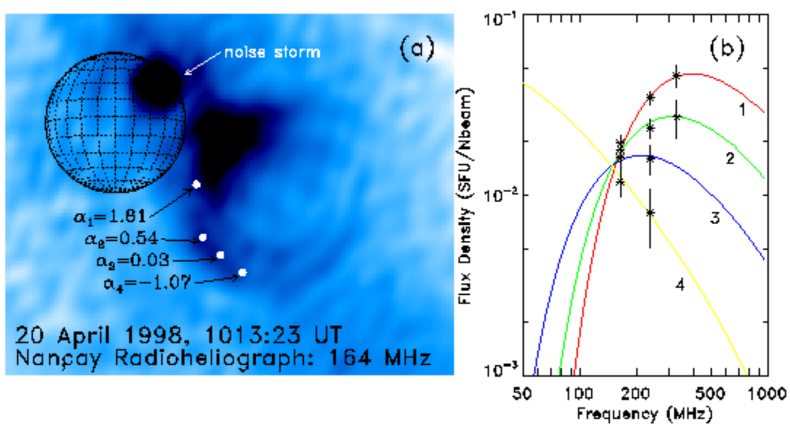

LoS	α	R_{sun}	ϕ (deg)	n_e (cm^{-3})	B(G)	ν_{RT} (MHz)
1	1.81	1.45	234	2.5×10^7	1.47	330
2	0.54	2.05	218.5	1.35×10^7	1.03	265
3	0.03	2.4	219.5	6.5×10^6	0.69	190
4	-1.07	2.8	221	5×10^5	0.33	30